Imaging Transverse Flow Velocity Using Spectral Bandwidth of the Doppler Frequency Shift in Phase-resolved ODT

Hongwu Ren, Zhongping Chen*, Kjell Morten Brecke, Zhihua Ding,
Yonghua Zhao, J. Stuart Nelson

Biomedical Engineering Center and Beckman Laser Institute,
University of California, Irvine, CA 92612

Abstract

The Doppler bandwidth extracted from the standard deviation of the frequency shift in phase-resolved optical Doppler tomography (ODT) is used to image the velocity component transverse to the probing beam. Using a simple geometric optics model, the linear dependence of the Doppler bandwidth on flow velocity is theoretically derived and it is found that the effective numerical aperture (NA) of the optical objective determines the slope of this dependence. Above a certain threshold flow velocity, this linear relationship is in good agreement with experimental data. In the case where the angle between the probing beam and flow direction is within ±15 degree to the perpendicular, the Doppler frequency shift is very sensitive to angle position while the Doppler bandwidth is insensitive to flow direction. Linear dependence of the flow velocity on the Doppler bandwidth allows accurate measurement of flow velocity without precise determination of flow direction. In addition, it also extends the dynamic range of the average frequency shift mapping method used in the phase-resolved ODT.

Keywords: phase-resolved optical Doppler tomography, Doppler bandwidth, transverse flow.

Introduction

Optical Doppler tomography (ODT) combines Doppler velocimetry with optical coherence tomography (OCT) [1] for noninvasive location and measurement of particle flow velocity in highly scattering media with micrometer-scale spatial resolution [2-6]. The principle employed in ODT is very similar to that used in radar, sonar and medical ultrasound. ODT uses a low coherence source and optical interferometer to obtain high spatial resolution gating with a high speed scanning device such as a rapid scanning optical delay line (RSOD) [7-8] to perform fast ranging of microstructure and particle motion detection in biological tissues or other turbid media. To detect the Doppler frequency shift signal induced by the moving particles, several algorithms and hardware schemes have been developed for ODT. The most straightforward method to determine the frequency shift is using of a small time fast Fourier transform (STFFT) [2-4]. However, the sensitivity of this method is mainly dependent on the FFT time window, which limits axial scanning speed and spatial resolution when measuring slowly moving blood flow in small vessels that requires high velocity sensitivity. However, a phase-resolved technique [5-6] can decouple the Doppler sensitivity and spatial resolution while maintaining high axial scanning speed. The limitation of phase-resolved ODT is that the dynamic range of the Doppler frequency shift measured is small because of an aliasing phenomenon caused by 2π ambiguity in the arctangent function. In our previous paper [6] on phase-resolved ODT, we reported on the use of the standard deviation of the Doppler spectrum to locate the microvasculature. In this paper, we demonstrate that standard deviation of the Doppler spectrum can also provide quantitative information on flow velocity. Using a simple geometric optics model, the linear dependence of the

* Correspondence: Email: hren@laser.bli.uci.edu or zchen@bli.uci.edu; WWW: http://www.bli.uci.edu/; Telephone: 949-824-4713; Fax: 949-824-8413

Coherence Domain Optical Methods in Biomedical Science and Clinical Applications VI,
Valery V. Tuchin, Joseph A. Izatt, James G. Fujimoto, Editors, Proceedings of SPIE
Vol. 4619 (2002) © 2002 SPIE · 1605-7422/02/$15.00

Doppler bandwidth on the flow velocity is theoretically derived and it is found that the effective numerical aperture (NA) of the optical objective in the sample arm determines the slope of this dependence. When flow velocity is much higher than that of the Brownian motion of the moving particle, the linear dependence of the flow velocity on the Doppler bandwidth allows accurate measurement of flow velocity transverse to the optical axis of the probing light beam.

Principle of Transverse Velocity Measurement

Phase-resolved ODT solves the compromise between spatial resolution and velocity sensitivity in the STFFT algorithm by mapping the phase change between sequential A-line signals for velocity detection. Phase-resolved ODT increases the imaging frame rate and it also increases the sensitivity of flow velocity detection by more than 2 orders of magnitude. The complex analytical function $\tilde{\Gamma}_j(t)$ of each A-line ODT digitized fringe signal $\Gamma_j(t)$ is calculated by the Hilbert transform

$$\tilde{\Gamma}_j(t) = \Gamma_j(t) + i\mathrm{H}\{\Gamma_j(t)\} = A(t)e^{i\psi(t)} \tag{1}$$

where H, A, ψ, j and t denotes the Hilbert transform, the amplitude and phase of the complex function $\tilde{\Gamma}_j(t)$, A-line number and RSOD group delay time, respectively. The average Doppler frequency shift and standard deviation of the Doppler spectrum for each pixel can be obtained simultaneously by the following equation, respectively,

$$f_D(k) = \frac{1}{2\pi T}\tan^{-1}\left(\frac{\mathrm{Im}\left[\sum_{j=1}^{n}\tilde{\Gamma}_j(k)\cdot\tilde{\Gamma}^*_{j+1}(k)\right]}{\mathrm{Re}\left[\sum_{j=1}^{n}\tilde{\Gamma}_j(k)\cdot\tilde{\Gamma}^*_{j+1}(k)\right]}\right) \tag{2}$$

$$\sigma(k) = \sqrt{\frac{\int_{-\infty}^{+\infty}(f-f_D)^2P(f)df}{\int_{-\infty}^{+\infty}P(f)df}} = \frac{1}{2\pi}\sqrt{\frac{2}{T^2}\left(1-\frac{\left|\sum_{j=1}^{n}\tilde{\Gamma}_j(k)\cdot\tilde{\Gamma}^*_{j+1}(k)\right|}{\sum_{j=1}^{n}\tilde{\Gamma}_j(k)\cdot\tilde{\Gamma}^*_{j}(k)}\right)} \tag{3}$$

where k is the pixel index, T is the A-line scanning period, Im denotes imaginary part and Re denotes real part of the complex value, f is the Doppler frequency shift, $P(f)$ is Doppler power spectrum. From equation (2), the velocity limit known as 2π ambiguity velocity range is obtained as,

$$V_{\max}^{f_d} = \frac{\lambda}{4\cos\theta}f_s \tag{4}$$

Equation (4) indicates that the maximum unambiguous velocity $V_{\max}^{f_d}$ detected by the phase-resolved method is determined by the RSOD scanning speed f_s, the center wavelength of the optical source λ and cosine of the Doppler angle θ.

There are a number of factors that contribute to the broadening of the Doppler spectrum including Brownian motion, velocity gradient and turbulence and focusing beam geometry of the optical probing beam, which is not plane wave.

When velocity is high, probing beam geometry dominates the broadening of the Doppler spectrum. The contribution from the focusing beam geometry can be derived from the optical geometry as show in Figure 1. When the Doppler angle larger than $\tan^{-1}(2w/l_c)$, where w is waist radius of the optical Gausian beam at the focus point and l_c is the optical coherence length, the Doppler bandwidth is determined by the difference between two extreme average Doppler frequency shift caused by the two optical rays at the two boundaries of the probing optical beam. The average Doppler frequency shift corresponding to these two optical rays can be written as

$$f_a = \frac{2V\cos(\theta - \phi)}{\lambda} \tag{5}$$

$$f_b = \frac{2V\cos(\theta + \phi)}{\lambda} \tag{6}$$

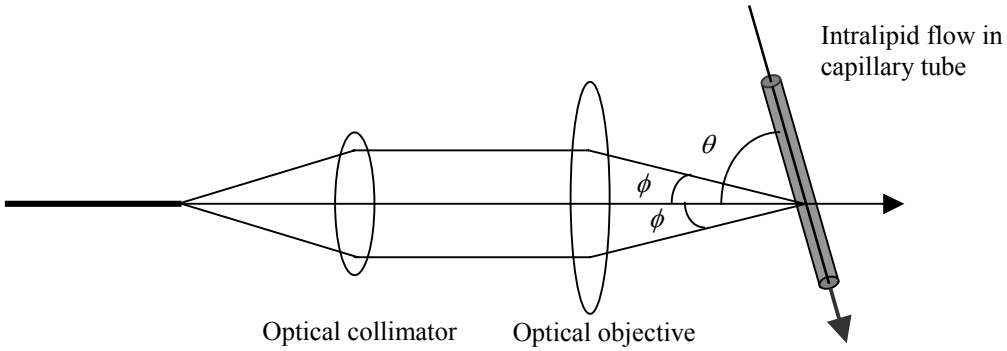

Figure 1. Probe beam geometry in the sample arm. θ is the Doppler angle between the optical axis and the flow velocity direction.

The estimated bandwidth of the Doppler signal derived from the above two equations is

$$B_d = f_a - f_b = \frac{4V}{\lambda}\sin\phi\sin\theta = \frac{4V\sin\theta NA_{eff}}{\lambda} \tag{7}$$

In this equation, B_d is the Doppler bandwidth, V is the flow velocity, ϕ is the optical aperture angle, θ is the Doppler angle and, NA_{eff} is the effective numerical aperture. The Doppler bandwidth B_d is defined by the above geometrical optics method. For a Gaussian optical beam, the Doppler bandwidth $B_{1/e}$ (full width at $1/e$ of maximum spectrum amplitude) is the inverse of the transit time spent by particles passing through the focus zone of the Gaussian optical beam. The relationship between $B_{1/e}$ and B_d is:

$$B_{1/e} = \frac{\pi}{8}B_d \tag{8}$$

Considering the relationship between the standard deviation and the Doppler bandwidth for a Gaussian optical beam,

$$B_{1/e} = 4\sigma \tag{9}$$

the relationship between the standard deviation and NA_{eff} can be derived as,

$$\sigma = \frac{\pi V \sin\theta NA_{eff}}{8\lambda} \tag{10}$$

If we include the contributions from Brownian motion and other factors that are independent of the macroscopic flow velocity, equation (10) can be modified as,

$$\sigma = \frac{\pi V \sin\theta NA_{eff}}{8\lambda} + b \tag{11}$$

where b accounts for bandwidth spectrum broadening from all of these sources. From the above theoretical result, the standard deviation is linearly dependent on velocity above a background value, and the effective numerical aperture NA_{eff} of the optical objective in the sample arm determines the slope of this velocity dependence. Knowing NA_{eff}, the measurement of the standard deviation can be used to determine the flow velocity. The flow velocity detected by the Doppler bandwidth method will be limited by the aliasing phenomenon being described by $\sigma \le f_s$. However, because the Doppler bandwidth and standard deviation are much smaller than the average frequency shift in the flow conditions encountered in most case, the Doppler bandwidth can extend the detection range of flow velocity. The range of velocity detection using the Doppler bandwidth method is determined by,

$$V_{\max}^{\sigma} \sin\theta = \frac{8\lambda(f_s - b)}{\pi NA_{eff}} \tag{12}$$

From equations (4) and (12), we can determine the ratio of the range of velocity detection for these two methods when they are directly applied with no phase unwrapping methods used,

$$M = \frac{V_{\max}^{\sigma}}{V_{\max}^{f_d}} = \frac{32}{\pi NA_{eff} \tan\theta}\left(1 - \frac{b}{f_s}\right) \tag{13}$$

The experiment system used for the Doppler bandwidth measurement has been previously described [5-6]. The optical source for the fiber interferometer is a low coherence ASE broadband source, whose output power, center wavelength, and bandwidth is 5 mW, 1300 nm and 65 nm, respectively. The source is coupled to the source arm and split into reference and sample arms by a 3-dB 2×2 coupler. A rapid-scanning optical delay line (RSOD) in a group delay scanning mode is used for 500 Hz A-line scanning, and an E-O phase modulator at 500 kHz with a ramp signal is used as a carrier frequency producer to implement a heterodyne detection scheme. In the sample arm shown in Figure 1, an exchangeable optical collimator and an optical objective ($20\times$, $N.A.,0.35$) are used to focus the optical beam to the center of a capillary tube whose inner diameter is 900 μm for M-mode imaging. A 0.1% intralipid solution composed of particles (0.356 micrometer diameter) is used as the turbid media, and a syringe pump driven by a high-resolution translation stage controls its flow through the capillary tube. In the detection arm, the signal from the photodector is amplified with a bandpass preamplifier and then sent to a A-D conversion and data acquisition board sampling at 5 MHz, the number of data points for each A-line data acquisition is 4096. The A-line scanning of RSOD, phase modulation of the E-O phase modulator and data acquisition of the data acquisition board are synchronized in order to get precise alignment of the original phase of the sequential A-line scans.

Results and Analysis

The standard deviation images of the intralipid flow in the center section of the capillary tube for different NA_{eff}, Doppler flow angle θ are captured for a velocity from 0 to 960 $\mu m/s$. The position of the focus point of the optical probing beam is fixed to the center of the tube. The profiles of the flow standard deviation images for three velocities are shown in Figure 2. We extract the center part of every flow standard deviation profile for a velocity from 0 to 960 $\mu m/s$ to study the relationship between Doppler bandwidth and velocity. The extracted result from the center part of every standard deviation profile corresponds to the top of the parabolic flow profile in the tube. The experimental standard deviation data and theoretical curves from equation (11) are shown in Figure 3 when NA_{eff} equals 0.09 and 0.05 at Doppler angle 77°. The solid and dotted lines are the theoretical curves and experiment results respectively. The theoretical and experimental curves are in good agreement for velocities higher than 300 $\mu m/s$. For NA_{eff} equals 0.09 and 0.05, the background b is 66 and 64.5 Hz, respectively. At low flow velocity, the standard deviation is constant. This is because at low velocity Brownian motion, which is independent of the macroscopic flow velocity, dominates the Doppler bandwidth. The regime for velocities higher than 300 $\mu m/s$ is dominated by Doppler bandwidth broadening originated from the optical beam geometry. Figure 3 indicates that the slope of the Doppler bandwidth dependence on velocity is proportional to NA_{eff}. The standard deviation experimental data and theoretical calculations for different angles and two NA_{eff} values 0.09 and 0.05 at a velocity of 698 $\mu m/s$ are shown in Figure 4. Figure 4 indicates that the dependence of Doppler bandwidth is insensitive to Doppler angles around 90°. The background b when the effective NA equals 0.09 and 0.05 is 65.6 and 64.8 Hz, respectively. Therefore the Doppler bandwidth component in the standard deviation can be used in this situation to measure transverse velocity. It can be used in intravascular imaging blood flow using endoscopic optical coherence tomography where the Doppler angle is around 90°, and most of the blood vessels are parallel to the surface of the skin, so this method has its merit for this reason. From Figure 3, it was determined that there is no aliasing phenomenon even though the velocity has reached 960 $\mu m/s$, which is much higher than the largest measurable velocity with the average Doppler frequency shift mapping method described by equation (4). This is because the standard deviation is only a small fraction of the average Doppler frequency shift as explained by equation (13). The ratio M theoretical curves are plotted in Figure 5 for two different NA_{eff}. Figure 5 indicates that the unambiguous detection range of velocities using the Doppler bandwidth mapping method can be many (10~20) times larger than the corresponding average Doppler frequency shift mapping method when the Doppler angle is in the range from 70° to 85°. Therefore the Doppler bandwidth mapping method is a promising tool for overcoming the 2π ambiguity of velocity detection in the average Doppler frequency shift mapping method.

Conclusion

In conclusion, the Doppler bandwidth can be used to measure flow velocity transverse to the probing beam direction. Using a geometric optics model, the linear dependence of the Doppler bandwidth on flow velocity is theoretically derived and it is found that the slope of this dependence is determined by the NA_{eff} of the optical objective. Above a certain threshold flow velocity, this linear relationship is in good agreement with experimental data. In the case where the angle between the probing optical beam and flow direction is within ± 15 degree to the perpendicular, the average Doppler frequency shift is very sensitive to angle position while the Doppler bandwidth is insensitive to flow direction. Linear dependence of the flow velocity on the Doppler bandwidth allows accurate measurement of flow velocity without precise determination of flow direction. Finally, this technique also extends the dynamic range of the average Doppler frequency shift mapping method used in the phase-resolved ODT.

Acknowledgements

This work was supported by research grants awarded from National Institutes of Health (HL-64218, RR-01192 and GM-58785) and National Science Foundation (BES-86924). Institutional support from the Air Force Office of Scientific

Research (N00014-94-1-0874), Department of Energy (DE-FG03-91ER61227), and the Beckman Laser Institute Endowment is also gratefully acknowledged.

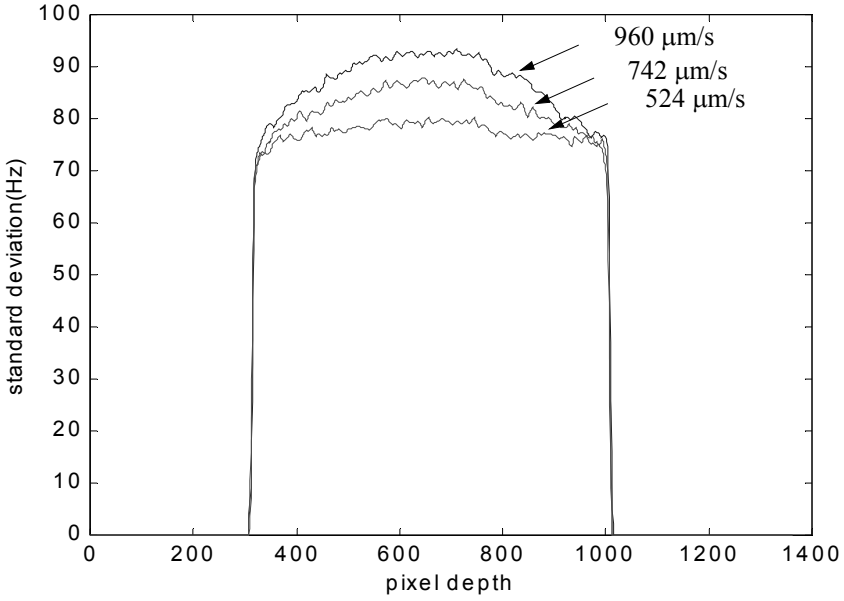

Figure 2. Standard deviation flow profile in the center of the capillary

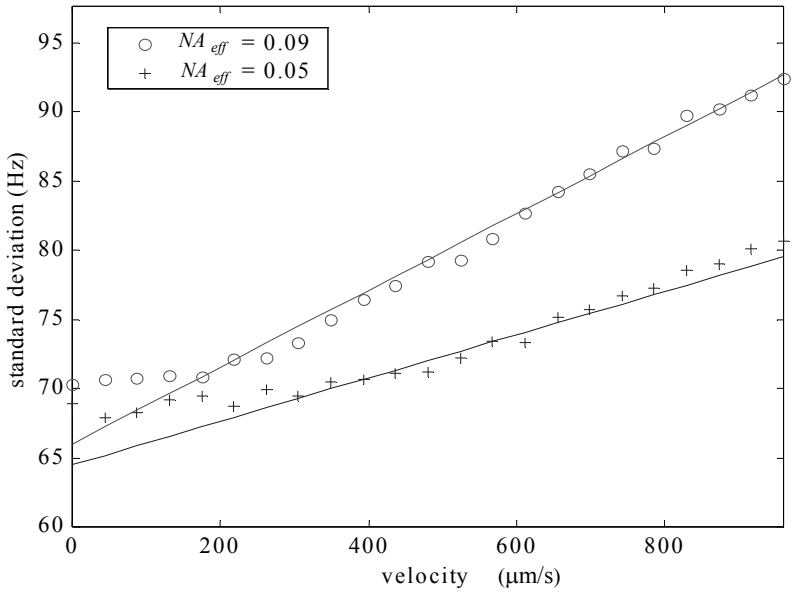

Figure 3. Standard deviation dependence on velocity and NA_{eff} at Doppler angle 77 degree$^{\circ}$, the solid line is theoretical curve from equation (11). For NA_{eff} equals 0.09 and 0.05, the background b is 66 and 64.5 Hz, respectively.

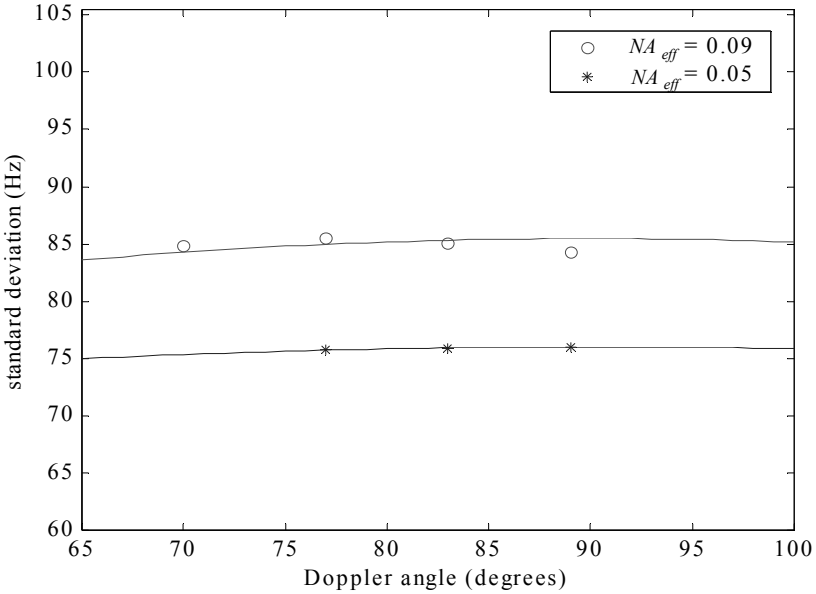

Figure 4. Standard deviation at different Doppler flow angles for two NA_{eff} 0.09 and 0.05 when the flow velocity is 698 $\mu m / s$. The background b when the effective NA equals 0.09 and 0.05 is 65.6 and 64.8 Hz, respectively.

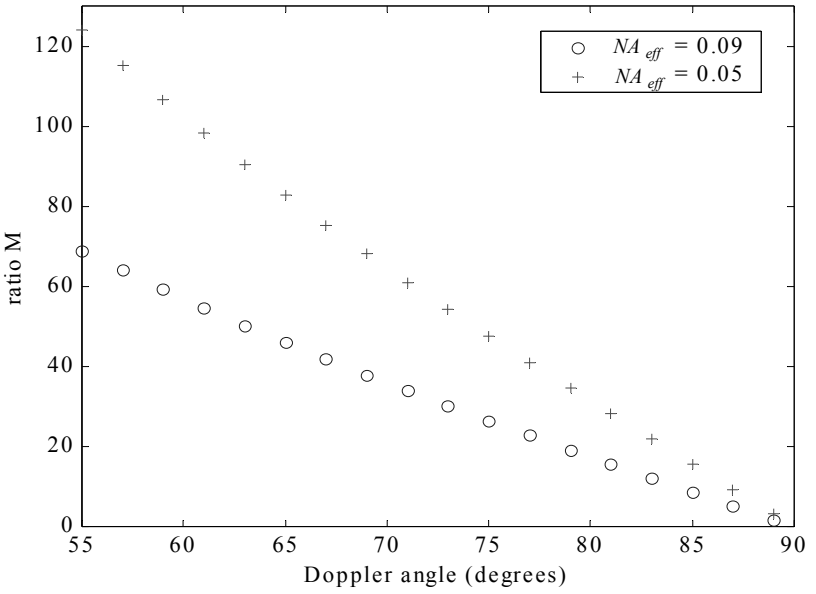

Figure 5. Ratio of the detection range of velocity by the Doppler bandwidth and average frequency shift mapping methods. The scanning frequency rate of the RSOD is 500, and the background of standard deviation b is 70 Hz, which corresponds to the value determined in our experiment.

References

1. D. Huang, E. A. Swanson, C. P. Lin, J. S. Schuman, W. G. Stinson, W. Chang, M. R. Hee, T. Flotte, K. Gregory, C. A. Puliafito and J. G. Fujimoto, Science 254, 1178 (1991).
2. Z. Chen, T. E. Milner, D. Dave and J. S. Nelson, Opt. Lett. 22, 64 (1997).
3. Z. Chen, T. E. Milner, S. Srinivas, X. Wang, A. Malekafzali, M. J. C. van Gemert and J. S. Nelson, Opt. Lett. 22, 1119 (1997).
4. M. D. Kulkarni, T. G. van Leeuwen, S. Yazdanfar and J. A. Izatt, Opt. Lett. 23, 1057 (1998).
5. Y. Zhao, Z. Chen, C. Saxer, S. Xiang, J. F. de Boer and J. S. Nelson, Opt. Lett. 25, 114(2000)
6. Y. Zhao, Z. Chen, C. Saxer, Q. Shen, S. Xiang, J. F. de Boer and J. S. Nelson, Opt. Lett. 25, 1358(2000)
7. G. J. Tearney, B. E. Bouma and J. G. Fujimoto, Opt. Lett. 22, 1811 (1997).
8. A. M. Rollins, M. D. Kulkarni, S. Yazdanfar, R. Ung-arunyawee and J. A. Izatt, Optics Express 3, 219 (1998)